International Journal of Mechatronics, Electrical and Computer Technology

**Vol. 4(12)**, Jul, 2014, pp. 886-909, **ISSN**: 2305-0543

Available online at: http://www.aeuso.org



# Effects of Variable Specific Heats of the Working Fluid, Internal Irreversibility, Heat Transfer and Friction on Performance of a Miller Cycle

A. Mousapour [1] and K. Rezapour [2*]

[1] Young Researchers and Elite Club, Karaj Branch, Islamic Azad University, Karaj, Iran.

[2] Department of Mechanical Engineering, Islamic Azad University, Karaj Branch, Karaj, Iran.

*Corresponding Author's E-mail: rezapour@kiau.ac.ir

## Abstract

In this paper, the performance of an irreversible Miller cycle is investigated. In the irreversible cycle, the linear relation between the specific heat of the working fluid and its temperature, the internal irreversibility described by using the compression and expansion efficiencies, the friction loss computed according to the mean velocity of the piston and the heat-transfer loss are considered. In addition to these irreversibilities, the effects of various design parameters, such as the minimum and maximum temperatures of the working fluid and the supplementary compression ratio on variation curves of the thermal efficiency versus the compression ratio, the power output versus the compression ratio and the power output versus the thermal efficiency are discussed. Now a day, Miller cycle is widely used in the automotive industry and the results obtained in this paper will provide some theoretical guidance for the design optimization of the Miller cycle.

**Keywords:** Miller cycle, Performance, Irreversibility, Specific heat, Compression ratio.

## 1. Introduction

The Miller cycle, named after R. H. Miller (1890-1967), is a modern modification of the Atkinson cycle and has an expansion ratio greater than the compression ratio. This is accomplished, however, in a much different way. Whereas an engine designed to operate on the Atkinson cycle needed a complicated mechanical linkage system of some kind, a

Miller cycle engine uses unique valve timing to obtain the same desired results. The cycle experienced in the cylinder of an internal combustion engine is very complex; to make the analysis of an engine cycle much more manageable, the real cycle is approximated with an ideal air-standard cycle, which differs from the actual by some aspects. In practice, the air-standard analysis is quite useful for illustrating the thermodynamic aspects of an engine operation cycle. Additionally, it can provide approximate estimates of trends as the major engine operating variables change. For the air-standard analysis, air (as an ideal gas with constant specific heats) is treated as the fluid flow through the entire engine, and property values of air are used in the analysis. The real open cycle is changed into a closed cycle by assuming that the amount of mass remains constant; combustion and exhaust strokes are replaced with the heat addition and heat rejection processes, respectively; and actual engine processes are approximated with ideal processes [1-4].

There are heat losses during the cycle of an actual engine that strongly affect the engine performance, but they are neglected in the air-standard analysis. In recent years, much attention has been paid to effect of the heat transfer on performance of internal combustion engines for different cycles. Klein [5] examined the effect of heat transfer through a cylinder wall on the work outputs of the Otto and Diesel cycles. Chen et al. [6, 7], Akash [8] and Hou [9] studied the effect of heat transfer through a cylinder wall during combustion on the net work output and the thermal efficiency of the air-standard Otto, Diesel and Dual cycles. Hou [10] also applied to performance analysis and comparison of air-standard Otto and Atkinson cycles with heat transfer consideration. In addition to heat losses, there is some friction between the piston and cylinder walls which is neglected in the air-standard analysis. Chen et al. [11] and Wang et al. [12] modeled the behaviors of Diesel and Dual cycles, with friction losses, over a finite period. Chen et al. [13] and Ge et al. [14] analyzed the performance of the air-standard dual and Miller cycles with heat transfer loss and friction-like term loss by using finite-time thermodynamics. Moreover, the

**Vol. 4(12)**, Jul, 2014, pp. 886-909, **ISSN**: 2305-0543
Available online at: http://www.aeuso.org


specific heats of the working fluid will not be constant during the engine operation cycles. Al-Sarkhi et al. [15] evaluated the performance of a Miller engine under different specific models (i.e., constant, linear, and fourth order polynomial). Ge et al. [16, 17], Chen et al. [18], Al-Sarkhi et al. [19, 20] investigated the effects of heat transfer, friction and variable specific heats of the working fluid on the performance of the Dual, Atkinson, Diesel and Miller cycles, respectively. The effects of heat loss as percentage of fuel's energy, friction and variable specific heats of the working fluid on the performance of the Otto, Atkinson, Miller and Diesel cycles have been analyzed by Lin and Hou [21-24]. In addition to above irreversibilities, the effect of internal irreversibility described by using compression and expansion efficiencies on the performance of Otto and dual cycles is investigated by Ge et al. [25, 26].

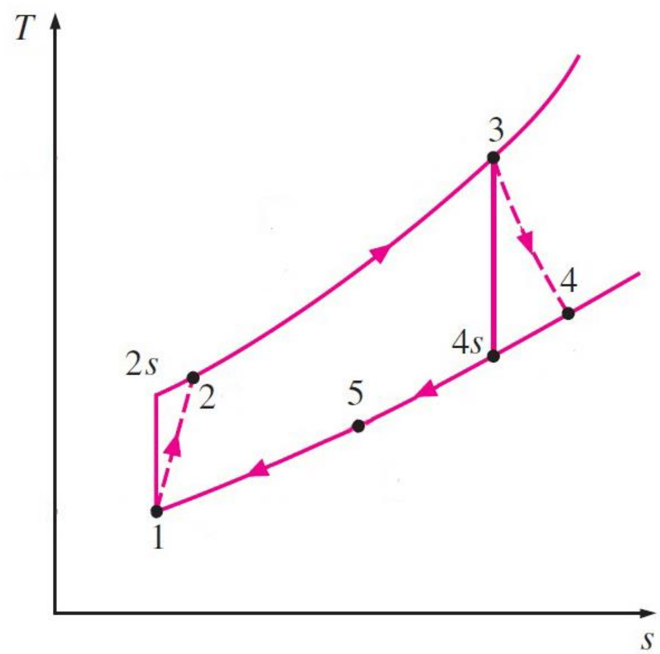


**Figure 1.** The *T-s* diagram of an air-standard Miller cycle [3].

International Journal of Mechatronics, Electrical and Computer Technology

**Vol. 4(12)**, Jul, 2014, pp. 886-909, **ISSN**: 2305-0543

Available online at: http://www.aeuso.org



## 2. Thermodynamic analysis

Since thermodynamic analysis of internal combustion engines in practical conditions is too complicated, for this reason, the real cycles are approximated with ideal air-standard cycles by applying a number of assumptions. The $T-s$ diagram of an air-standard Miller cycle are shown in figure 1. Process 1→2s is reversible adiabatic compression. Process 2s→3 is isochoric heat addition. Process 3→4s is reversible adiabatic expansion and processes 4s→5 and 5→1 are isochoric and isobaric heat rejection, respectively. In the air-standard analysis, the working fluid is assumed that to behave as an ideal gas with constant specific heats. But, this assumption can be valid only for the small temperature ranges during the cycle. For the large temperature range of 300→2000 K, this assumption cannot be applied, because it causes considerable errors. Hence, with a suitable approximation, the specific heats of the working fluid can be written as following linear functions of temperature [20]:

$$C_{\mathrm{P}} = a_{\mathrm{P}} + k_1 T, \tag{1}$$

and

$$C_{\mathrm{V}} = b_{\mathrm{V}} + k_1 T, \tag{2}$$

where, $C_{\mathrm{P}}$ and $C_{\mathrm{V}}$ are specific heats of the working fluid at constant pressure and volume, respectively. $a_{\mathrm{P}}$, $b_{\mathrm{V}}$ and $k_1$ are constants. Accordingly, the working fluid constant, R, will be equal to:

$$R = C_{\mathrm{P}} - C_{\mathrm{V}} = a_{\mathrm{P}} - b_{\mathrm{V}} \cdot \tag{3}$$

Equation describing entropy change for a reversible process is, as follow:

$$\int_{\mathrm{i}}^{\mathrm{j}} \mathrm{d}s = \int_{\mathrm{i}}^{\mathrm{j}} C_{\mathrm{V}} \frac{\mathrm{d}T}{T} + \int_{\mathrm{i}}^{\mathrm{j}} R \frac{\mathrm{d}V}{V} \cdot \tag{4}$$

Using Equations (2) and (4), for the isentropic processes (1→2s) and (3→4s), we will have:

**Vol. 4(12)**, Jul, 2014, pp. 886-909, **ISSN**: 2305-0543
Available online at: http://www.aeuso.org


$$k_1 \; T_{2s} - T_1 \; + b_V \ln\left(\frac{T_{2s}}{T_1}\right) - R \ln \; r_c \; = 0, \tag{5}$$

and

$$k_1 \; T_3 - T_{4s} \; + b_V \ln\left(\frac{T_3}{T_{4s}}\right) - R \ln \; r \, r_c \; = 0, \tag{6}$$

where, $T_1$ and $T_3$ are equal to the minimum and maximum temperatures of the working fluid; and $r_c$ and $r$ are the compression ratio and the supplementary compression ratio, respectively, that are defined as:

$$r_c = \frac{V_1}{V_2}, \tag{7}$$

and

$$r = \frac{V_5}{V_1}. \tag{8}$$

As it can be seen, in the ideal air-standard Miller cycle, for the reversible adiabatic compression (1→2s) and expansion (3→4s) processes, the entropy generation and thus the entropy change of the working fluid is zero, while in a real Miller cycle, the irreversibilities cause the entropy of the working fluid to increase, during the irreversible adiabatic compression (1→2) and expansion (3→4) processes. Therefore, the following compression and expansion efficiencies can be used to describe the internal irreversibilities of the compression and expansion processes, respectively [25, 26]:

$$\eta_c = \frac{T_{2s} - T_1}{T_2 - T_1}, \tag{9}$$

and

$$\eta_e = \frac{T_3 - T_4}{T_3 - T_{4s}}. \tag{10}$$

**International Journal of Mechatronics, Electrical and Computer Technology**

**Vol. 4(12)**, Jul, 2014, pp. 886-909, **ISSN**: 2305-0543

Available online at: http://www.aeuso.org



Assuming that the heat engine is operated at the rate of $N$ cycle per second, the heat added per second to the working fluid during the process 2→3 can be written as:

$$Q_{\mathrm{in}} = NM\int_{T_2}^{T_3} C_{\mathrm{V}}\,\mathrm{d}T = NM\int_{T_2}^{T_3} \left(b_{\mathrm{V}} + k_1 T\right)\mathrm{d}T = NM\left[0.5k_1\left(T_3^2 - T_2^2\right) + b_{\mathrm{V}}\left(T_3 - T_2\right)\right]\cdot \quad (11)$$

The heat rejected per second by the working fluid during processes 4→5 and 5→1 can be written as:

$$Q_{\mathrm{out}} = NM\left[\int_{T_5}^{T_4} C_{\mathrm{V}}\,\mathrm{d}T + \int_{T_1}^{T_5} C_{\mathrm{P}}\,\mathrm{d}T\right] = NM\left[\int_{T_5}^{T_4}\left(b_{\mathrm{V}} + k_1 T\right)\mathrm{d}T + \int_{T_1}^{T_5}\left(a_{\mathrm{P}} + k_1 T\right)\mathrm{d}T\right]$$
$$= NM\left[0.5k_1\left(T_4^2 - T_1^2\right) + b_{\mathrm{V}}\left(T_4 - T_5\right) + a_{\mathrm{P}}\left(T_5 - T_1\right)\right], \quad (12)$$

where, $M$ is the mass of the working fluid. The temperatures within the combustion chamber of an internal combustion engine reach values on the order of 2700 ($K$) and up. Materials in the engine cannot tolerate this kind of temperature and would quickly fail if proper heat transfer did not occur. Thus, because of keeping an engine and engine lubricant from thermal failure, the interior maximum temperature of the combustion chamber must be limited to much lower values by heat fluxes through the cylinder wall during the combustion period. Since, during the other processes of the operating cycle, the heat flux is essentially quite small and negligible due to the very short time involved for the processes, it is assumed that the heat loss through the cylinder wall occurs only during combustion. The calculation of actual heat transfer through the cylinder wall occurring during combustion is quite complicated, so it is approximately assumed to be proportional to the average temperature of both the working fluid and cylinder wall and that, during the operation, the wall temperature remains approximately invariant. Therefore, the heat leak per second is given by the following linear relation [16]:

$$Q_{\mathrm{Leak}} = NM\left[K\left(\frac{T_2 + T_3}{2} - T_0\right)\right] = NM\,B\left(T_2 + T_3 - 2T_0\right), \quad (13)$$

where, $K = 2B$ is the thermal conductance between the working fluid and the cylinder

International Journal of Mechatronics, Electrical and Computer Technology

**Vol. 4(12)**, Jul, 2014, pp. 886-909, **ISSN**: 2305-0543

Available online at: http://www.aeuso.org



wall, $B$ is a constant related to heat transfer and $T_0$ is the average temperature of the wall.

Thus, the total heat released by combustion can be obtained as:

$$Q_{\text{Total}} = Q_{\text{in}} + Q_{\text{Leak}} \cdot \tag{14}$$

Taking into account the friction loss of the piston and assuming a dissipation term represented by a friction force, which in a linear function of the piston velocity, gives [11, 12]:

$$f_{\mu} = \mu v = \mu \frac{\mathrm{d}x}{\mathrm{d}t}, \tag{15}$$

where, $\mu$ is a coefficient of friction, which takes into account the global losses, and $x$ is the piston position. Then, the lost power is:

$$P_{\mu} = \frac{\mathrm{d}W_{\mu}}{\mathrm{d}t} = f_{\mu} \frac{\mathrm{d}x}{\mathrm{d}t} = \mu \frac{\mathrm{d}x}{\mathrm{d}t} \frac{\mathrm{d}x}{\mathrm{d}t} = \mu v^2 \cdot \tag{16}$$

For the Miller engine, running at $N$ cycle per second, the mean velocity of the piston is:

$$\bar{v} = 4LN = 4N\ \ x_4 - x_3\ \ = 4N x_3\ \ r r_c - 1\ \ , \tag{17}$$

where, $L$ is the piston stroke and $x_3$ and $x_4$ are the piston positions at minimum and maximum volumes respectively. Finally, the power output and the thermal efficiency of the cycle will be obtained as:

$$P_{\text{output}} = Q_{\text{in}} - Q_{\text{out}} - P_{\mu}, \tag{18}$$

and

$$\eta_{\text{th}} = \frac{P_{\text{output}}}{Q_{\text{Total}}} \cdot \tag{19}$$

International Journal of Mechatronics, Electrical and Computer Technology
Vol. 4(12), Jul, 2014, pp. 886-909, ISSN: 2305-0543
Available online at: http://www.aeuso.org


## 3. Results and discussion

According to references [21-26], the following constants and parameters have been used in the calculations:

$M = 0.00126\ (kg)$ , $N = 30\ (cycle/s)$ , $T_{min} = 280-320\ (K)$ , $T_{max} = 1800-2200\ (K)$ , $r = 1.2-1.8$ , $k_1 = 0.000133-0.000271\ (kJ\ /kg\ K^2)$ , $a_P = 0.6858-0.8239 (kJ\ /kg\ K)$ , $b_V = 0.9728-1.1109\ (kJ\ /kg.K)$ , $R = 0.278\ (kJ\ /kg.K)$ , $\eta_c = 0.98$ , $\eta_e = 0.98$ , $B = 0.2-0.4\ (kJ\ /kg.K)$ , $\mu = 0.0129-0.0169\ (kN\,s\ /m)$, $x_3 = 0.01\ (m)$.

Substituting above constants and parameters into obtained equations and then choosing a suitable range for the compression ratio, $r_c$, we can get ranges of temperature of different states, the heat added per second, the heat rejected per second, the heat leakage, the total heat released by combustion per second, the power output and the thermal efficiency, in the specified range.

Figures 2-9 indicate the effects of parameters $T_{min}$, $T_{max}$, $r$, $\eta_c$, $\eta_e$, $B$, $a_P$, $b_V$, $k_1$ and $\mu$ on variation curve of the thermal efficiency versus the compression ratio. It can be seen that the thermal efficiency increases with increasing the compression ratio, reaches a maximum value and then decreases. According to these figures, the thermal efficiency increases with the increase of $T_{max}$, $r$, $\eta_c$ and $\eta_e$, and the decrease of $T_{min}$, $B$, $a_P$, $b_V$, $k_1$ and $\mu$, for a fixed compression ratio. Note that the effects of parameters $r$, $a_P$, $b_V$, $k_1$ will change with increasing the compression ratio. In addition, the maximum thermal efficiency increases with increasing $T_{max}$, $\eta_c$ and $\eta_e$, and decreasing $T_{min}$, $B$, $a_P$, $b_V$, $k_1$

International Journal of Mechatronics, Electrical and Computer Technology
**Vol. 4(12)**, Jul, 2014, pp. 886-909, **ISSN**: 2305-0543
Available online at: http://www.aeuso.org


and $\mu$. Moreover, with increasing $T_{\min}$, $r$, $B$ and $\mu$ and, decreasing $T_{\max}$, $\eta_c$, $\eta_e$, $a_P$, $b_V$, $k_1$, the maximum thermal efficiency occurs at smaller compression ratio.

Figures 10-17 show the effects of parameters $T_{\min}$, $T_{\max}$, $r$, $\eta_c$, $\eta_e$, $B$, $a_P$, $b_V$, $k_1$ and $\mu$ on variation curve of the power output versus the compression ratio. It can be seen that the power output increases with increasing the compression ratio, reaches a maximum value and then decreases. According to these figures, the power output increases with the increase of $T_{\max}$, $r$, $\eta_c$, $\eta_e$, $a_P$, $b_V$ and $k_1$, and the decrease of $T_{\min}$ and $\mu$, for a fixed compression ratio (parameter $B$ has no effect on the power output of the cycle). Note that the effect of parameter $r$ will change with increasing the compression ratio. In addition, the maximum power output increases with increasing $T_{\max}$, $r$, $\eta_c$, $\eta_e$, $a_P$, $b_V$ and $k_1$,and decreasing $T_{\min}$ and $\mu$. Moreover, with increasing $T_{\min}$, $r$ and $\mu$ and, decreasing $T_{\max}$, $\eta_c$, $\eta_e$, $a_P$, $b_V$ and $k_1$, the maximum power output occurs at smaller compression ratio.

Figures 18-25 depict the effects of parameters $T_{\min}$, $T_{\max}$, $r$, $\eta_c$, $\eta_e$, $B$, $a_P$, $b_V$, $k_1$ and $\mu$ on variation curve of the power output versus the thermal efficiency. It can be seen that the corresponding thermal efficiency at maximum power output increases with the increase of $T_{\max}$, $\eta_c$ and $\eta_e$, and the decrease of $T_{\min}$, $B$, $a_P$, $b_V$, $k_1$ and $\mu$. Also, the corresponding power output at maximum thermal efficiency increases with increasing $T_{\max}$, $r$, $\eta_c$, $\eta_e$, $B$, $a_P$, $b_V$ and $k_1$, and decreasing $T_{\min}$ and $\mu$.

**Vol. 4(12)**, Jul, 2014, pp. 886-909, **ISSN**: 2305-0543
Available online at: http://www.aeuso.org


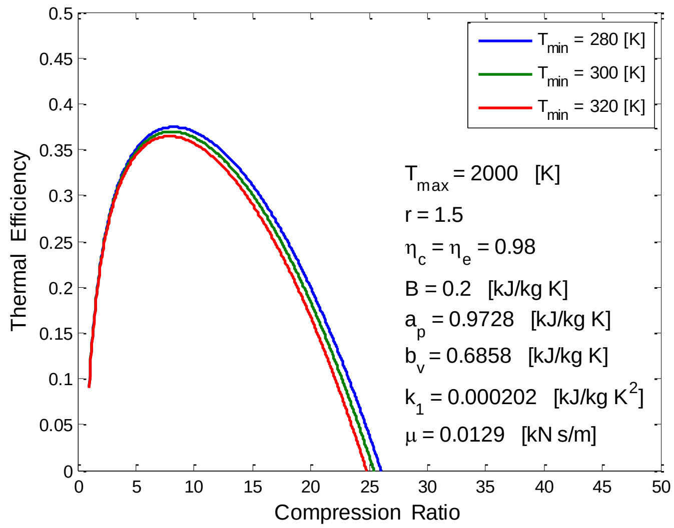


**Figure 2.** Effect of $T_{\min}$ on variation curve of the thermal efficiency versus the compression ratio.

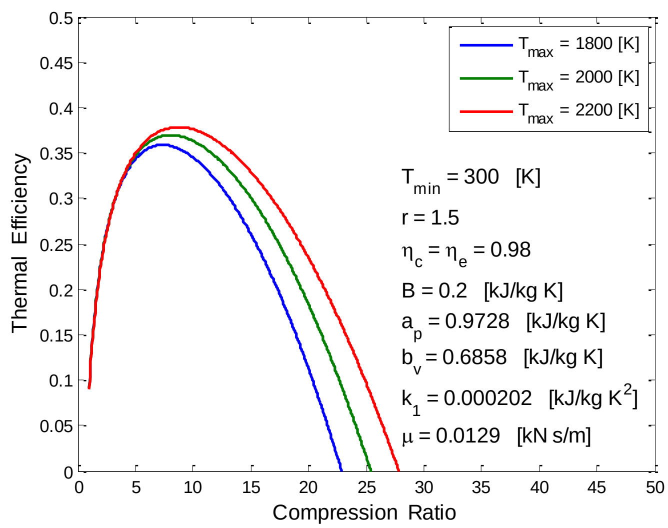


**Figure 3.** Effect of $T_{\max}$ on variation curve of the thermal efficiency versus the compression ratio.

International Journal of Mechatronics, Electrical and Computer Technology
**Vol. 4(12)**, Jul, 2014, pp. 886-909, **ISSN**: 2305-0543
Available online at: http://www.aeuso.org


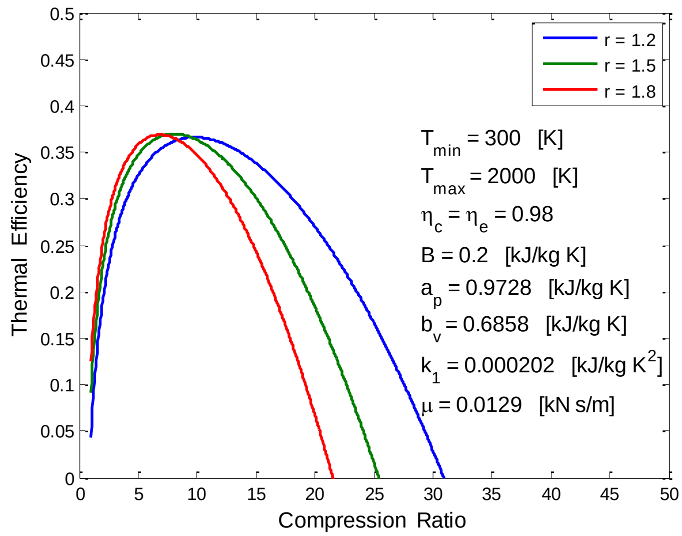


**Figure 4.** Effect of $r$ on variation curve of the thermal efficiency versus the compression ratio.

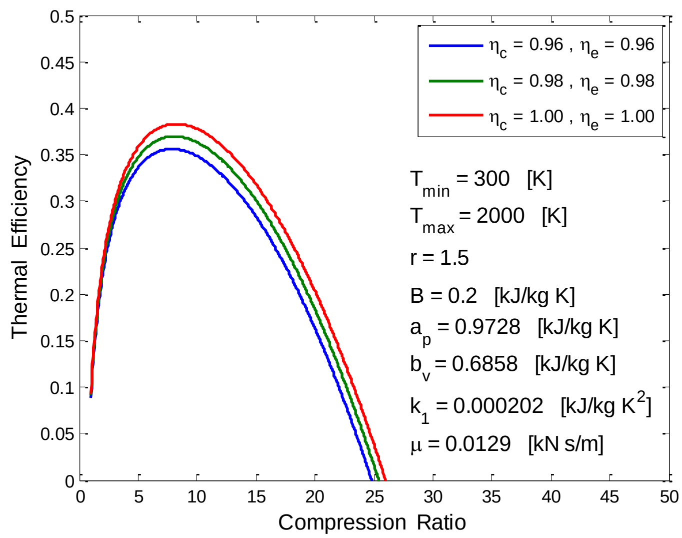


**Figure 5.** Effects of $\eta_c$ and $\eta_e$ on variation curve of the thermal efficiency versus the compression ratio.

International Journal of Mechatronics, Electrical and Computer Technology
**Vol. 4(12)**, Jul, 2014, pp. 886-909, **ISSN**: 2305-0543
Available online at: http://www.aeuso.org


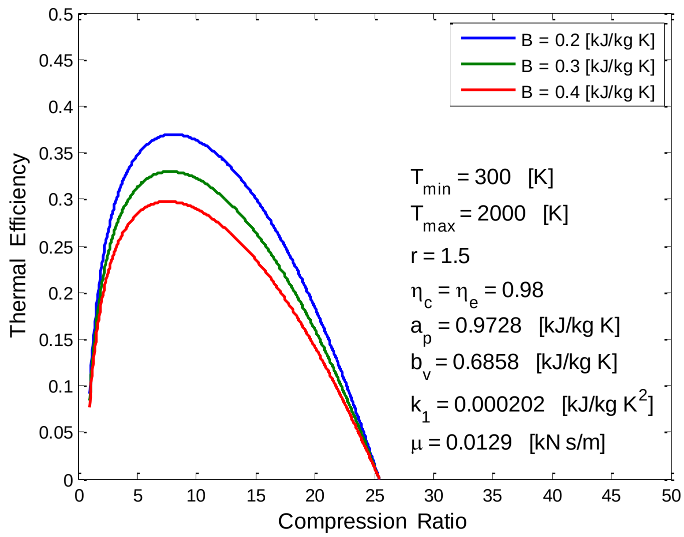


**Figure 6.** Effect of $B$ on variation curve of the thermal efficiency versus the compression ratio.

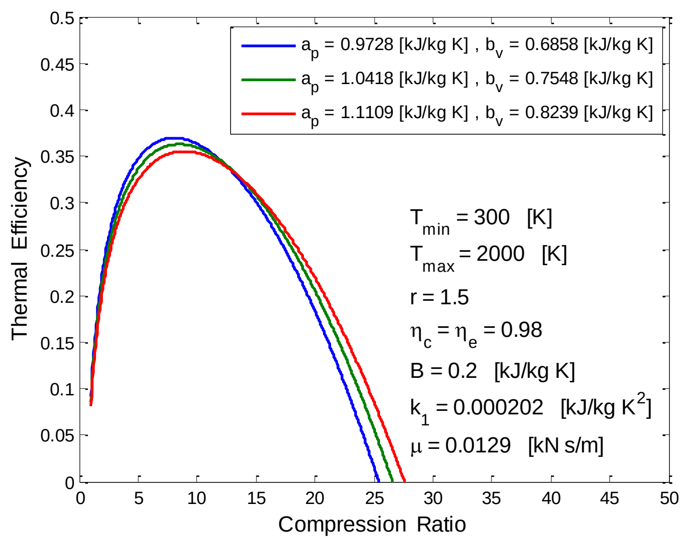


**Figure 7.** Effects of $a_p$ and $b_V$ on variation curve of the thermal efficiency versus the compression ratio.

International Journal of Mechatronics, Electrical and Computer Technology

**Vol. 4(12)**, Jul, 2014, pp. 886-909, **ISSN**: 2305-0543

Available online at: http://www.aeuso.org


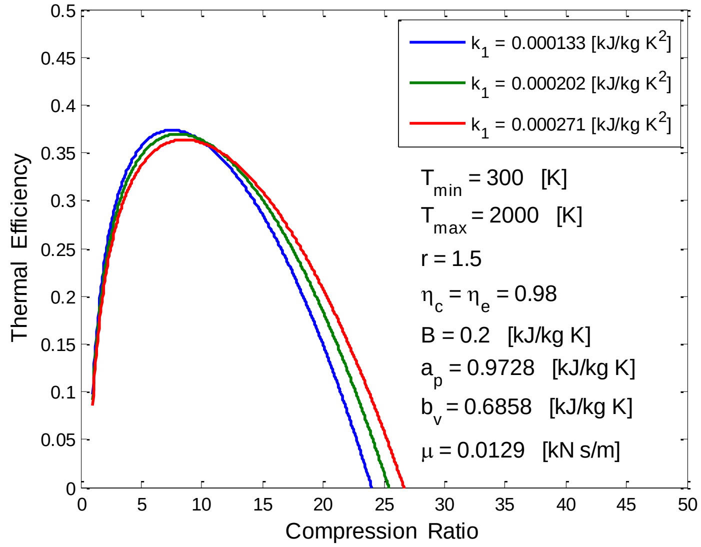


**Figure 8.** Effect of $k_1$ on variation curve of the thermal efficiency versus the compression ratio**.**

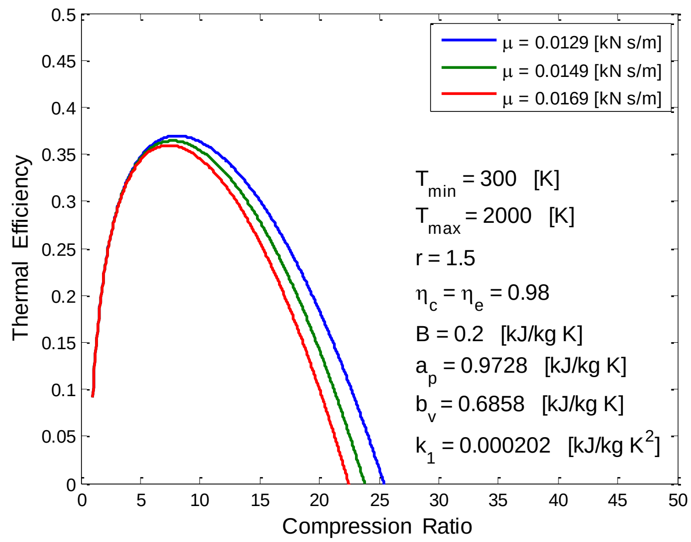


**Figure 9.** Effect of $\mu$ on variation curve of the thermal efficiency versus the compression ratio.

International Journal of Mechatronics, Electrical and Computer Technology
**Vol. 4(12)**, Jul, 2014, pp. 886-909, **ISSN**: 2305-0543
Available online at: http://www.aeuso.org


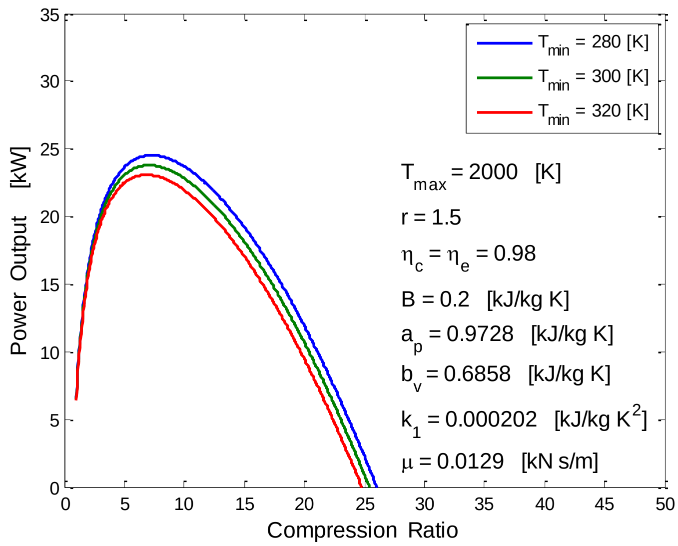


**Figure 10.** Effect of $T_{\min}$ on variation curve of the power output versus the compression ratio.

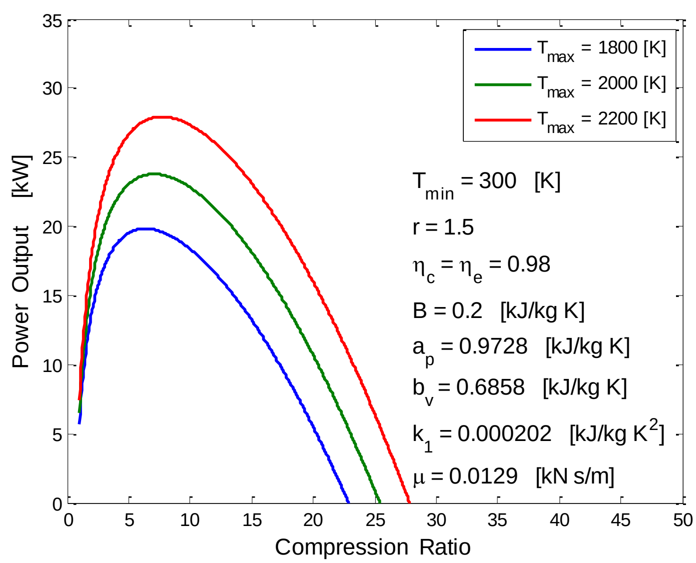


**Figure 11.** Effect of $T_{\max}$ on variation curve of the power output versus the compression ratio.

International Journal of Mechatronics, Electrical and Computer Technology
**Vol. 4(12)**, Jul, 2014, pp. 886-909, **ISSN**: 2305-0543
Available online at: http://www.aeuso.org


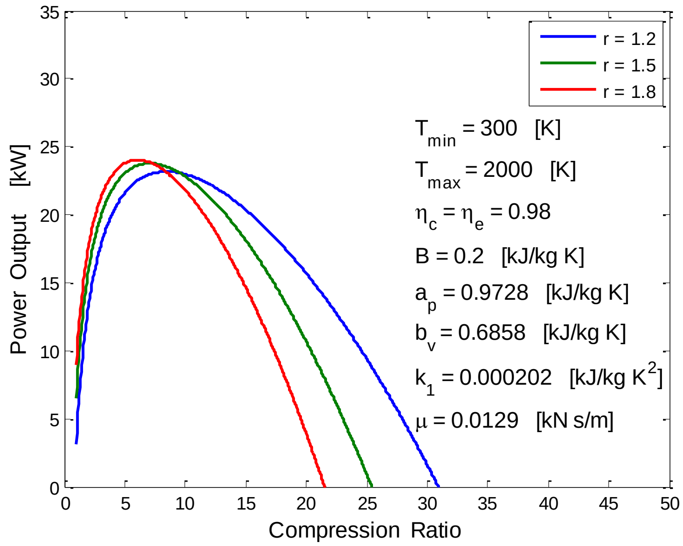


**Figure 12.** Effect of $r$ on variation curve of the power output versus the compression ratio.

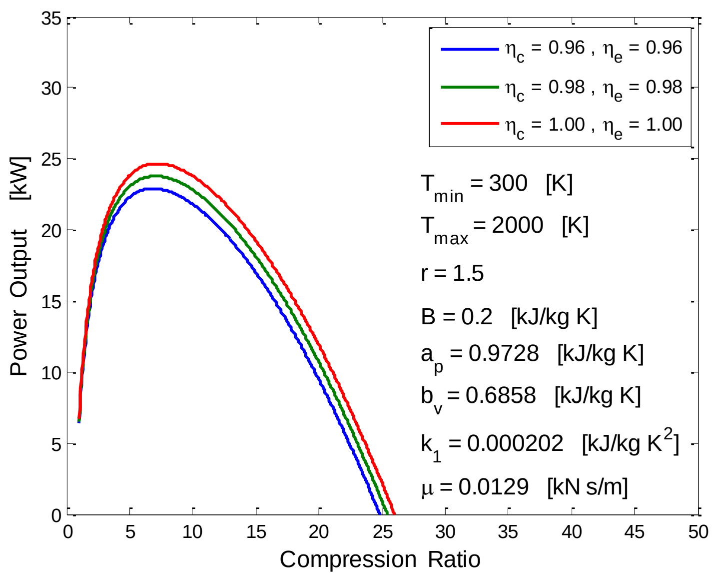


**Figure 13.** Effects of $\eta_c$ and $\eta_e$ on variation curve of the power output versus the compression ratio.

**Vol. 4(12)**, Jul, 2014, pp. 886-909, **ISSN**: 2305-0543
Available online at: http://www.aeuso.org


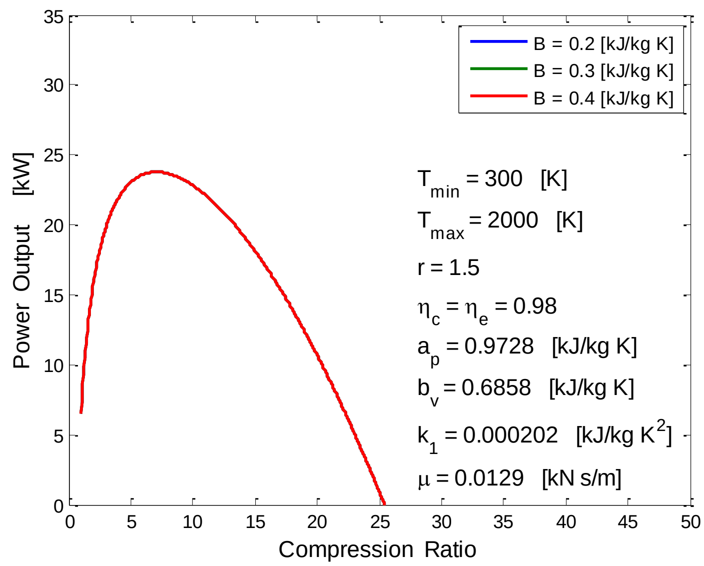


**Figure 14.** Effect of $B$ on variation curve of the power output versus the compression ratio.

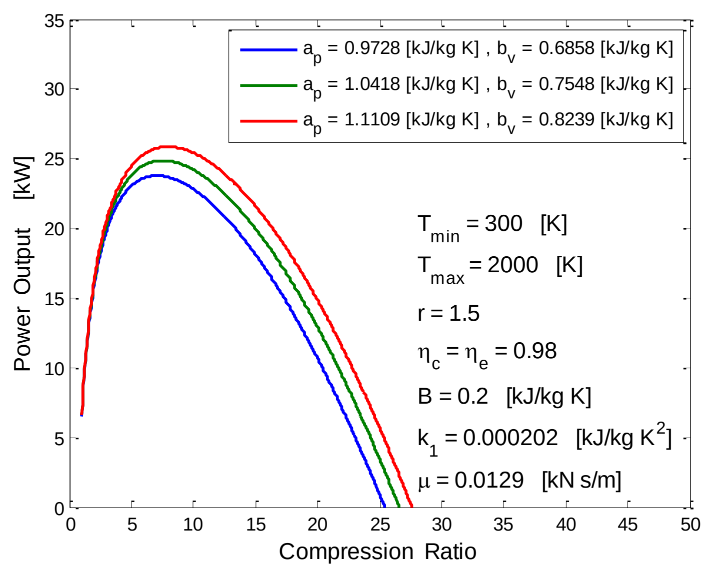


**Figure 15.** Effects of $a_p$ and $b_V$ on variation curve of the power output versus the compression ratio.

International Journal of Mechatronics, Electrical and Computer Technology

**Vol. 4(12)**, Jul, 2014, pp. 886-909, **ISSN**: 2305-0543

Available online at: http://www.aeuso.org



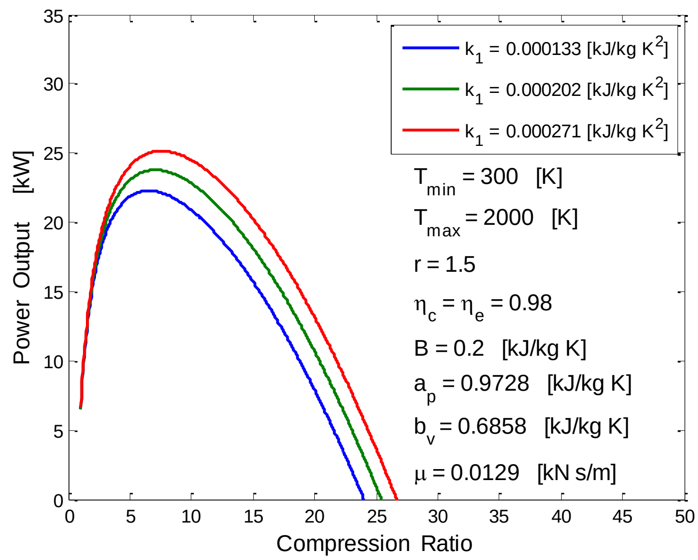


**Figure 16.** Effect of $k_1$ on variation curve of the power output versus the compression ratio.

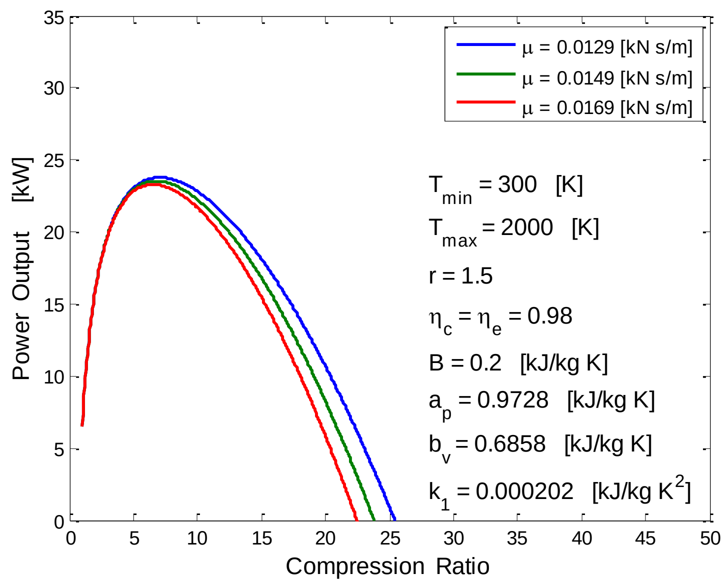


**Figure 17.** Effect of $\mu$ on variation curve of the power output versus the compression ratio.

International Journal of Mechatronics, Electrical and Computer Technology
Vol. 4(12), Jul, 2014, pp. 886-909, ISSN: 2305-0543
Available online at: http://www.aeuso.org


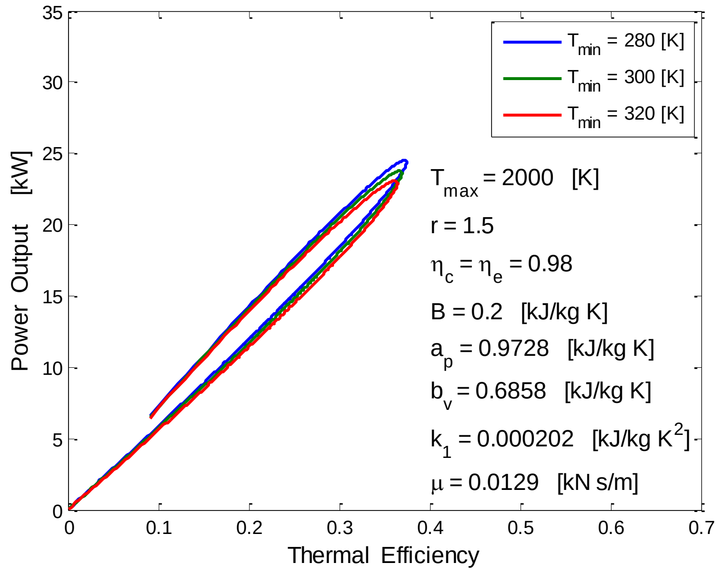


**Figure 18.** Effect of $T_{\min}$ on variation curve of the power output versus the thermal efficiency.

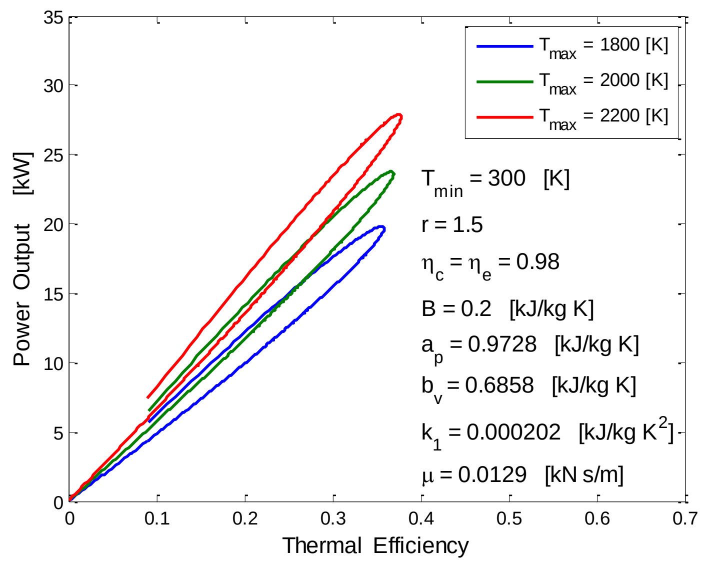


**Figure 19.** Effect of $T_{\max}$ on variation curve of the power output versus the thermal efficiency.

International Journal of Mechatronics, Electrical and Computer Technology

**Vol. 4(12)**, Jul, 2014, pp. 886-909, **ISSN**: 2305-0543

Available online at: http://www.aeuso.org



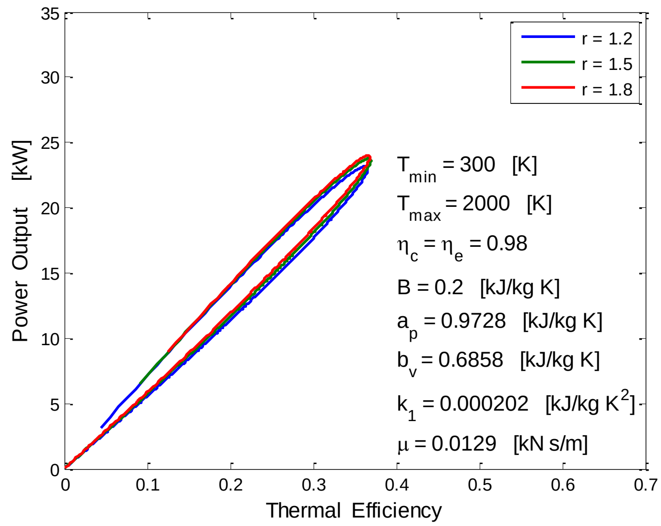


**Figure 20.** Effect of $r$ on variation curve of the power output versus the thermal efficiency.

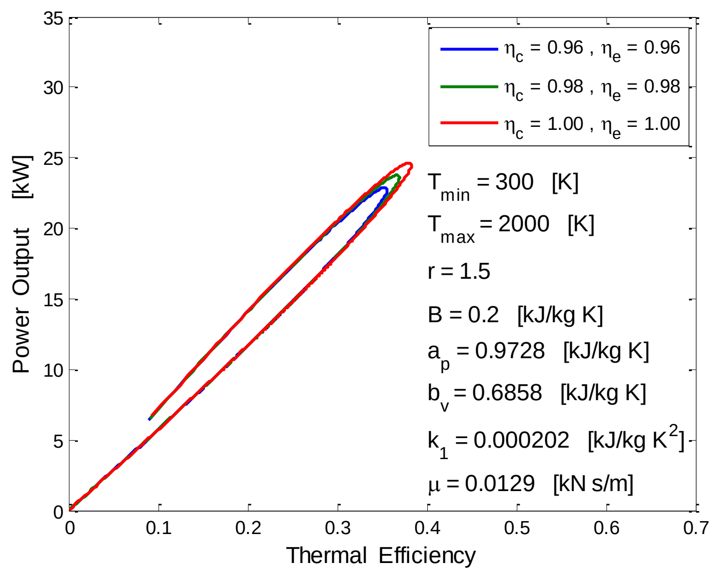


**Figure 21.** Effects of $\eta_c$ and $\eta_e$ on variation curve of the power output versus the thermal efficiency.

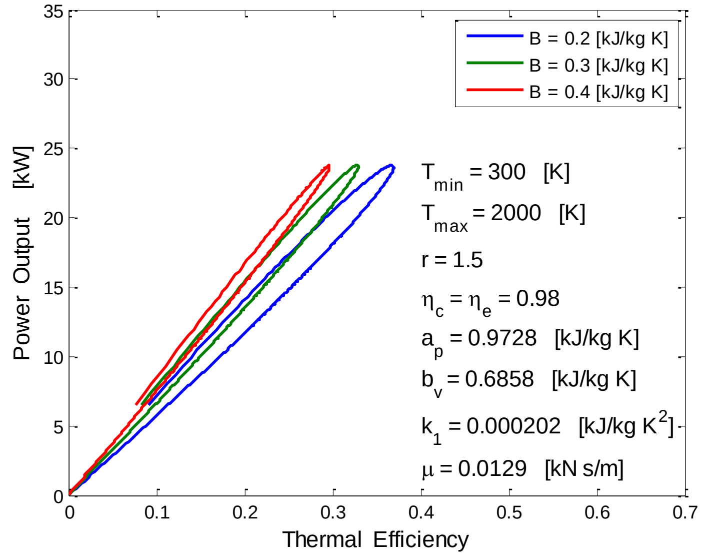


**Figure 22.** Effect of $B$ on variation curve of the power output versus the thermal efficiency.

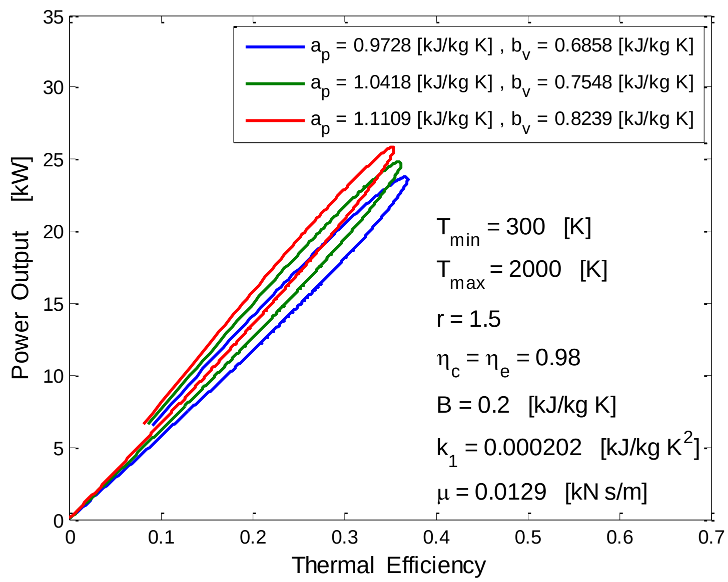


**Figure 23.** Effects of $a_P$ and $b_V$ on variation curve of the power output versus the thermal efficiency.

International Journal of Mechatronics, Electrical and Computer Technology

**Vol. 4(12)**, Jul, 2014, pp. 886-909, **ISSN**: 2305-0543

Available online at: http://www.aeuso.org


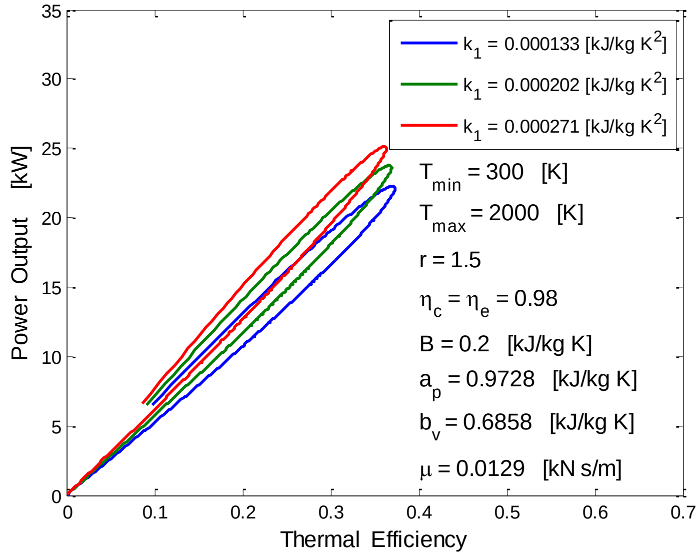


**Figure 24.** Effect of $k_1$ on variation curve of the power output versus the thermal efficiency.

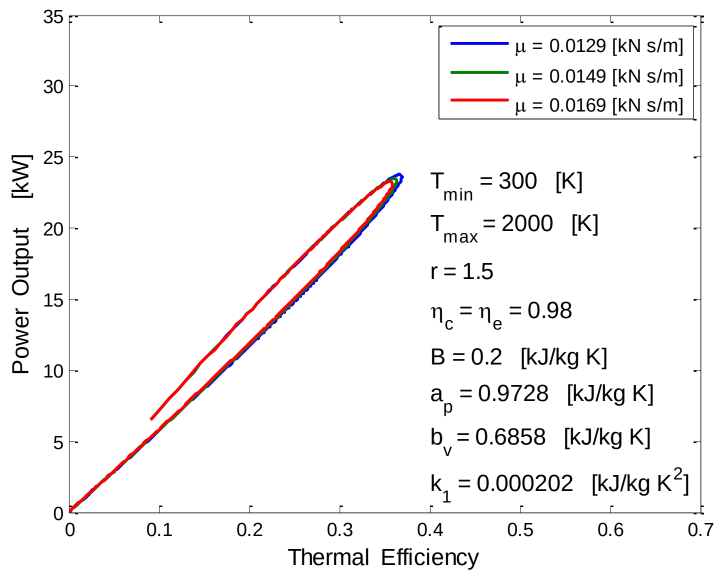


**Figure 25.** Effect of $\mu$ on variation curve of the power output versus the thermal efficiency.

**Vol. 4(12)**, Jul, 2014, pp. 886-909, **ISSN**: 2305-0543
Available online at: http://www.aeuso.org


## Conclusions

In this manuscript, performance of an air-standard Miller cycle with consideration of heat losses, friction losses, variable specific heats of the working fluid and internal irreversibility described by using compression and expansion efficiencies, is studied. Also, the effects of relevant parameters on variation curves of the thermal efficiency versus the compression ratio, the power output versus the compression ratio and the power output versus the thermal efficiency are indicated. The obtained results show that the effects of these parameters on the performance of the Miller cycle are non-negligible and should be considered in practical Miller engines.

## References

[1] W. W. Pulkrabek, Engineering fundamentals of the internal combustion engine, Prentice-Hall, New Jersey (1997).

[2] J. B. Heywood, Internal combustion engine fundamentals, McGraw-Hill, New York (1988).

[3] Y. A. Cengel, M. A. Boles, Thermodynamics: an engineering approach, 7th Ed, McGraw-Hill Book Company, (2010).

[4] A. Bejan, Advanced engineering thermodynamics, Hoboken, John Wiley & Sons INC, New Jersey (2006).

[5] S. A. Klein. An explanation for observed compression ratios in internal combustion engines. Journal of Engineering for Gas Turbines and Power, 113( 4), (1991), pp. 511-513.

[6] L. Chen, C. Wu, F. Sun, S. Cao. Heat transfer effects on the net work output and efficiency characteristics for an air standard Otto cycle. Energy Conversion and Management, 39(7), (1998), pp. 643-648.

[7] L. Chen, F. Zeng, F. Sun, C. Wu. Heat transfer effects on net work and/or power as functions of efficiency for air standard Diesel cycles. Energy, 21(12), (1996), pp. 1201-1205.

[8] B. Akash. Effect of heat transfer on the performance of an air standard Diesel cycle. International Communication in Heat and Mass Transfer, 28(1), (2001), pp. 87-95.

[9] S. S. Hou. Heat transfer effects on the performance of an air standard dual cycle. Energy Conversion and Management, 45(18/19), (2004), pp. 3003-3015.

**Vol. 4(12)**, Jul, 2014, pp. 886-909, **ISSN**: 2305-0543
Available online at: http://www.aeuso.org


[10] S. S. Hou. Comparison of performances of air standard Atkinson and Otto cycles with heat transfer considerations. Energy Conversion and Management, 48(5), (2007), pp. 1683-1690.

[11] L. Chen, J. Lin, J. Lou, F. Sun, C. Wu. Friction effect on the characteristic performance of Diesel engine. Energy, 26(10), (2002), pp. 965-971.

[12] W. Wang, L. Chen, F. Sun, C. Wu. The effect of friction on the performance of an air standard Dual cycle. Exergy, an International Journal, 2(4), (2002), pp. 340-344.

[13] L. Chen, F. Sun and C. Wu. Optimal performance of an irreversible Dual cycle. Applied Energy, 79(1), (2004), pp. 3-14.

[14] Y. Ge, L. Chen, F. Sun, C. Wu. Effects of heat transfer and friction on the performance of an irreversible air standard Miller cycle. International Communication in Heat and Mass Transfer, 32(8), (2005), pp. 1045-1056.

[15] A. Al-Sarkhi, J. Al-Hinti, E. Abu-Nada, B. Akash. Performance evaluation of irreversible Miller engine under various specific heat models. International Communication in Heat and Mass Transfer, 34(7), (2007), pp. 897-906.

[16] L. Chen, Y. Ge, F. Sun, C. Wu. Effects of heat transfer, friction and variable specific heats of working fluid on performance of an irreversible Dual cycle. Energy Conversion and Management, 47(18/19), (2006), pp. 3224-3234.

[17] Y. Ge, L. Chen, F. Sun, C. Wu. Performance of an Atkinson cycle with heat transfer, friction and variable specific heats of the working fluid. Applied Energy, 83(11), (2006), pp. 1210-1221.

[18] Y. Ge, L. Chen, F. Sun, C. Wu. Performance of a Diesel cycle with heat transfer, friction and variable specific heats of the working fluid. Journal of the Energy Institute, 80(4), (2007), pp. 239-242.

[19] A. Al-Sarkhi, J. O. Jabber, M. Abu-Qudais, S. D. Probert. Effects of friction, temperature dependent specific heat of the working fluid on the performance of a Diesel engine. Applied Energy, 83(2), (2006), pp. 153-165.

[20] A. Al-Sarkhi, J. O. Jabber, S. D. Probert. Efficiency of a Miller engine. Applied Energy, 83(4), (2006), pp. 343-351.

[21] J. C. Lin, S. S. Hou. Effects of heat loss as percentage of fuel's energy, friction and variable specific heats of working fluid on performance of air standard Otto cycle. Energy Conversion and Management, 49(5), (2008), pp. 1218-1227.

[22] J. C. Lin, S. S. Hou. Influence of heat loss on the performance of an air standard Atkinson cycle. Applied Energy, 84(9), (2007), pp. 904-920.

**Vol. 4(12)**, Jul, 2014, pp. 886-909, **ISSN**: 2305-0543
Available online at: http://www.aeuso.org


[23] J. C. Lin, S. S. Hou. Performance analysis of an air standard Miller cycle with considerations of heat loss as a percentage of fuel's energy, friction and variable specific heats of working fluid. International Journal of Thermal Sciences, 47(2), (2008), pp. 182-191.

[24] S. S. Hou, J. C. Lin. Performance analysis of a Diesel cycle under the restriction of maximum cycle temperature with considerations of heat loss, friction and variable specific heats. Academic Journal of Acta Physica Polonica, 120(6), (2011), pp. 979-986.

[25] Y. Ge, L. Chen, F. Sun. Finite time thermodynamic modeling and analysis for an irreversible Otto cycle. Applied Energy, 85(7), (2008), pp. 618-624.

[26] Y. Ge, L. Chen, F. Sun. Finite time thermodynamic modeling and analysis for an irreversible Dual cycle. Mathematical and Computer Modelling, 50(½), (2009), pp. 101-108.